# 8. Antiparallel β-Sheet Conformation in Cyclopeptides Containing a Pseudo-amino Acid with a Biphenyl Moiety

by **Volker Brandmeier**, **Wolfgang H. B. Sauer**, and **Martin Feigel***

Institut für Organische Chemie, Universität Erlangen-Nürnberg, Henkestr. 42, D–91054 Erlangen

(30.IX.93)

The biphenyl-containing pseudo-amino acids 2′-(aminomethyl)biphenyl-2-carboxylic acid (Abc; **1**) and 2′-(aminomethyl)biphenyl-2-acetic acid (Aba; **2**) are used as rigid spacers in the backbone of the cyclic peptides cyclo(-Abc-Ala-Phe-Gly-)$_2$ (**5**), cyclo(-Abc-Ala-Val-Gly-)$_2$ (**6**), cyclo(-Aba-Gly-Phe-Ala-)$_2$ (**7**), and cyclo(-Aba-Ala-Phe-Gly-)$_2$ (**8**). Three different interconverting diastereoisomers are found in solutions of each of these cyclopeptides due to the atropisomerism of the biphenyl units. NMR Techniques and molecular-dynamics calculations allow to conclude that the major diastereoisomer of **5** (and **6**) in ($D_6$)DMSO adopts a β-sheet conformation. It is proposed that the pseudo-amino acid **1** of (*R*)-chirality forms, with attached L-amino acids, a H-bonding pattern comparable to a β-turn (see **D** in *Fig. 4* and **F**).

**Introduction.** – Surrogates for the β-turn in peptides were investigated recently by several groups [1]. The research in this field is stimulated by the potent biological activity of small naturally occurring (cyclo)peptides where β-loops determine the geometry of parts of the molecules (some ref. are given in [2]). Artificial β-turns may induce the formation of β-sheets in attached peptides. Several small β-sheets, stabilized by artificial β-loops, may perhaps be assembled to large synthetic cavities with functional groups in chiral positions. The structure of these cavities would be comparable to the holes found in natural or synthetic β-barrel proteins [3].

We already reported on two cyclic peptides where the pseudo-amino acids **1** (Abc) [4] and **2** (Aba) [5] hold together two valine (Val) or two alanine (Ala) moieties in an antiparallel assembly as in **3**.

The X-ray structure of the Val derivative **4** corresponding to **3** confirms that the biphenyl unit **1** orients the small peptide fragments so that interchain H-bonds are built as in a β-sheet [4]. However, the pseudo-amino acid **1** does not mimic a β-loop in **4**. The H-bonding pattern resembles rather a δ-loop [6].

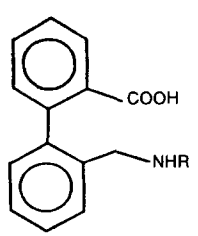


**1** R = H, Abc
**9** R = Boc

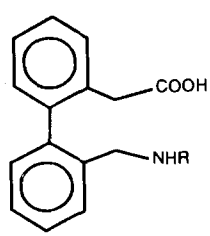


**2** R = H, Aba
**10** R = Boc

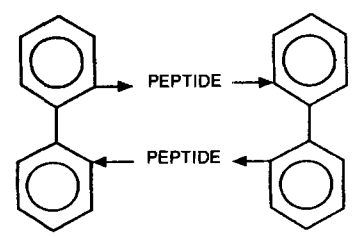


**3**

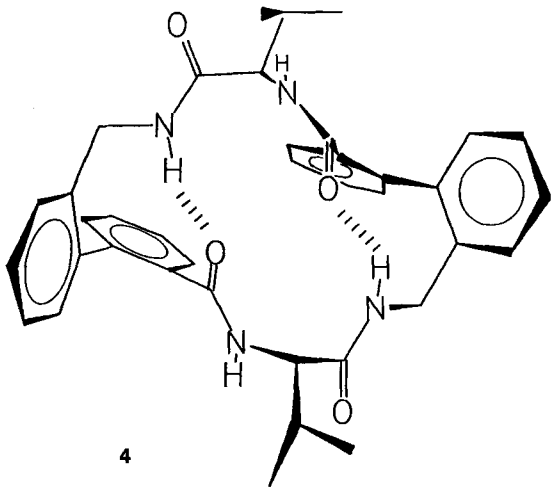

4

The constrained conformation in the solid state of **4** is maintained in solution [4]. The question is open whether **1** can induce a similar conformation in macrocycles with longer peptide chains. This paper reports the synthesis and conformational study of two such extended cycles, *i.e.* of compounds cyclo(-Abc-Ala-Phe-Gly-)$_2$ (**5**) and cyclo(-Abc-Ala-Val-Gly-)$_2$ (**6**). In addition, the synthesis of two cyclopeptides is described which contain the pseudo-amino acid **2**, *i.e.* of cyclo(-Aba-Gly-Phe-Ala-)$_2$ (**7**) and cyclo(-Aba-Ala-Phe-Gly-)$_2$ (**8**).

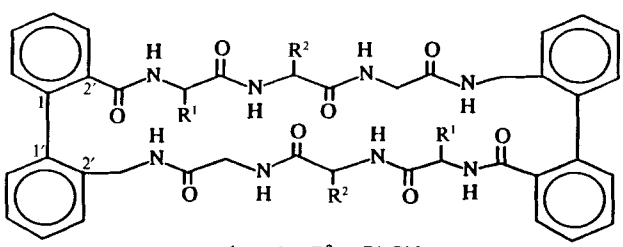

**5** $R^1$ = Me, $R^2$ = $PhCH_2$
**6** $R^1$ = Me, $R^2$ = i-Pr

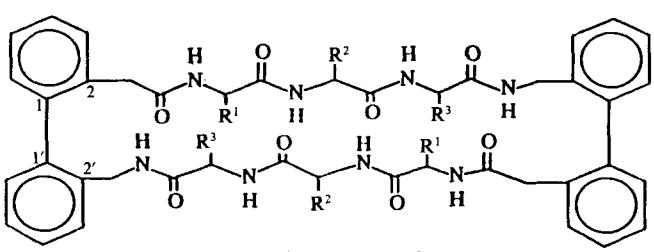

**7** $R^1$ = H, $R^2$ = $PhCH_2$, $R^3$ = Me
**8** $R^1$ = Me, $R^2$ = $PhCH_2$, $R^3$ = H

**Synthesis.** – The preparation of *N*-phthaloyl-protected derivatives of the pseudo-amino acids 2′-(aminomethyl)biphenyl-2-carboxylic acid ( = Abc; **1**) and 2′-(aminomethyl)biphenyl-2-acetic acid ( = Aba; **2**) was already reported [4] [5]. Cyclic peptides like compound **4** were obtained in these studies by cyclodimerization of the coupling product of **1** or **2** with the appropriate amino acid. This approach did not work in the preparation of the larger compounds **5–8**; monomers were isolated under similar conditions. However, the azide cyclization of linear precursors containing two biphenyl and two tripeptide units was successful, giving the 'dimeric' cyclic peptides **5–8** in low to moderate yields (3–17%).

The *Scheme* explains the synthesis: Tripeptide esters were condensed with *N*-[(*tert*-butoxy)carbonyl] (Boc) derivatives **9** or **10** of **1** and **2**, respectively (prepared from the corresponding *N*-phthaloyl derivatives) [5], using *N*-methylmorpholine (NMM) and propylphosphonic anhydride (PPA) [7] to yield the Boc-protected tetrapeptide methyl esters **11–14**. The N-terminal Boc group was removed with dioxane/2N HCl [8] in half of the material of these biphenyl-containing peptides, and the ester group was saponified with 1N NaOH [9] in the other half. The thus obtained fragments were condensed with NMM/PPA to yield the Boc-octapeptide methyl esters **15–18**. The protective groups were removed with $NH_2NH_2 \cdot H_2O$ and dioxane/2N HCl, respectively, and the resulting amino hydrazide was cyclized by the azide methode according to *Medzihradszky* [10], giving the target cyclic peptides **5–8**.

**$^1$H-NMR Studies of the Conformations of Peptides 5–8.** – If two biphenyl groups of (*R*)- or (*S*)-chirality are connected with flexible peptide chains containing L-amino acids, three diastereoisomers **A–C** of averaged $C_2$, $C_2$, and $C_1$ symmetry, respectively, are ex-

*Scheme*

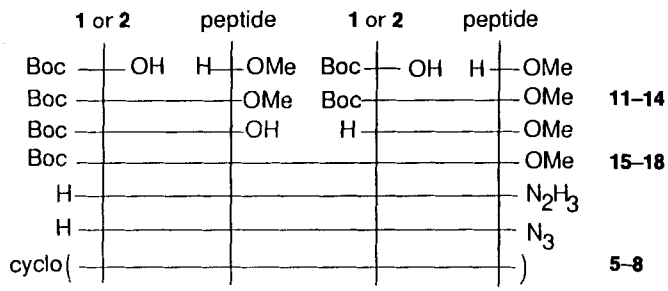


Boc-Abc-Ala-Phe-Gly-OMe **11**

Boc-Abc-Ala-Val-Gly-OMe **12**

Boc-Aba-Gly-Phe-Ala-OMe **13**

Boc-Aba-Ala-Phe-Gly-OMe **14**

Boc-(Abc-Ala-Phe-Gly-)$_2$OMe **15**

Boc-(Abc-Ala-Val-Gly-)$_2$OMe **16**

Boc-(Aba-Gly-Phe-Ala-)$_2$OMe **17**

Boc-(Aba-Ala-Phe-Gly-)$_2$OMe **18**

pected for the cyclic peptides **5–8** (see *Fig. 1*). Indeed, ($D_6$)DMSO solutions of **5–8** exhibit $^1$H-NMR signals of all three diastereoisomers **A–C**.

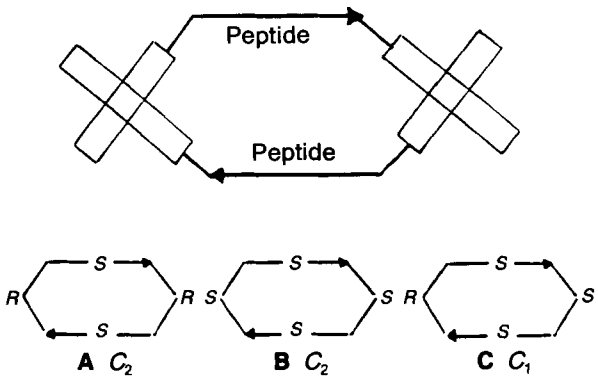


Fig. 1. *Diastereoisomers* **A–C** *of cyclic peptides of type* **5–8**

*Compounds* **5** *and* **6** *Containing the Biphenyl Bridge* **1**. A typical $^1$H-NMR spectrum of **5** in ($D_6$)DMSO is shown in *Fig. 2*. The dominating signals in the spectrum belong to a diastereoisomer of $C_2$ symmetry (see **A** or **B** in *Fig. 1*) and are assigned easily using the connectivities found in 2D-COSY spectra. The signals of the two remaining minor

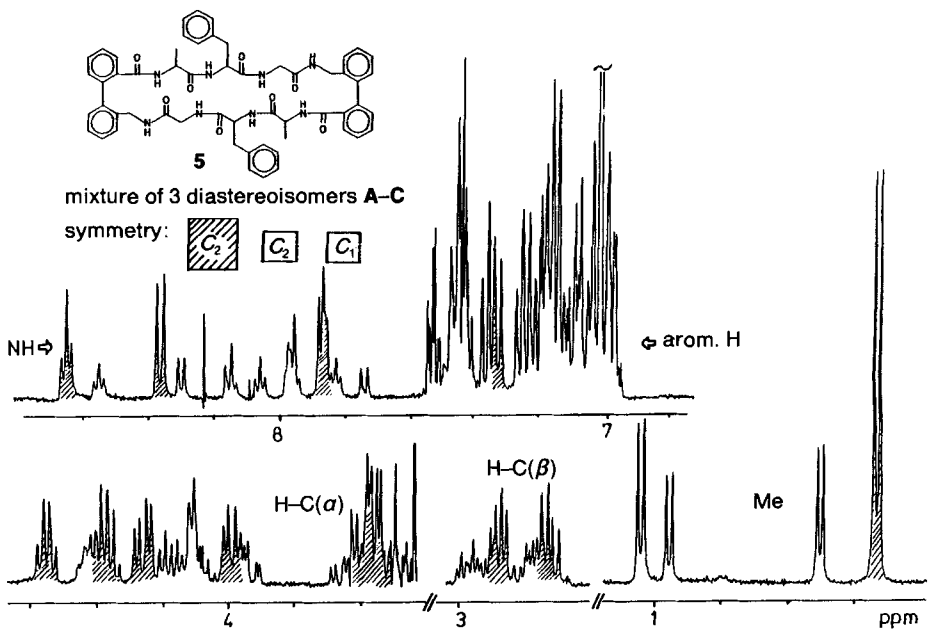


Fig. 2. *$^1$H-NMR Spectrum* (400 MHz) *of* **5** *in ($D_6$)DMSO at 35°*. Signals of the aliphatic CH and NH of the dominant atropisomer of $C_2$ symmetry are shaded.

isomers can also be located, but severe overlaps, both in the NH and in the H–C(α) region, prevent a complete analysis (*e.g.*, the CH and NH signals of the $CH_2NH$ groups of glycine of **5** do nearly coincide in the less populated isomers). Therefore, the following conformational evaluation is focussed on the dominant isomer having $C_2$ symmetry.

The major atropisomer of **5** in ($D_6$)DMSO seems also to be the structure found in the solid state of material which is recrystallized in MeCN. If solid **5** is dissolved at −30° in ($D_6$)DMSO/$CDCl_3$ 1:1 (*v/v*), the $^1$H-NMR recorded immediately afterwards shows only the broadened signals of the dominating $C_2$ form. A spectrum recorded at −15° a few min later contains already additional small signals of the remaining diastereoisomers, and the equilibration is complete after *ca.* 1 h at 25° giving approximately the isomer distribution shown in *Fig. 2* ($C_2$:$C_1$:$C_2$ = 1:0.7:0.2).

The chemical exchange between the different isomers is also observed in the 2D-ROESY spectra of **5** in ($D_6$)DMSO at 35° and at higher temperatures (see *Fig. 3*). The cross-peaks due to chemical exchange connect $^1$H signals in both $C_2$ forms with the corresponding signals in the $C_1$ form. Therefore, the process has to be described by the kinetic scheme **A** ⇄ **C** ⇄ **B**. Obviously, only one of the two biphenyl moieties isomerizes in one of the kinetic steps. A similar distribution of exchanging isomers with one dominant $C_2$ form is also found in ($D_6$)DMSO solutions of **6**.

Many conformationally relevant informations can easily be extracted from the $^1$H-NMR spectra of the dominant $C_2$ forms of **5** and **6**. *E.g.*, vicinal coupling constants

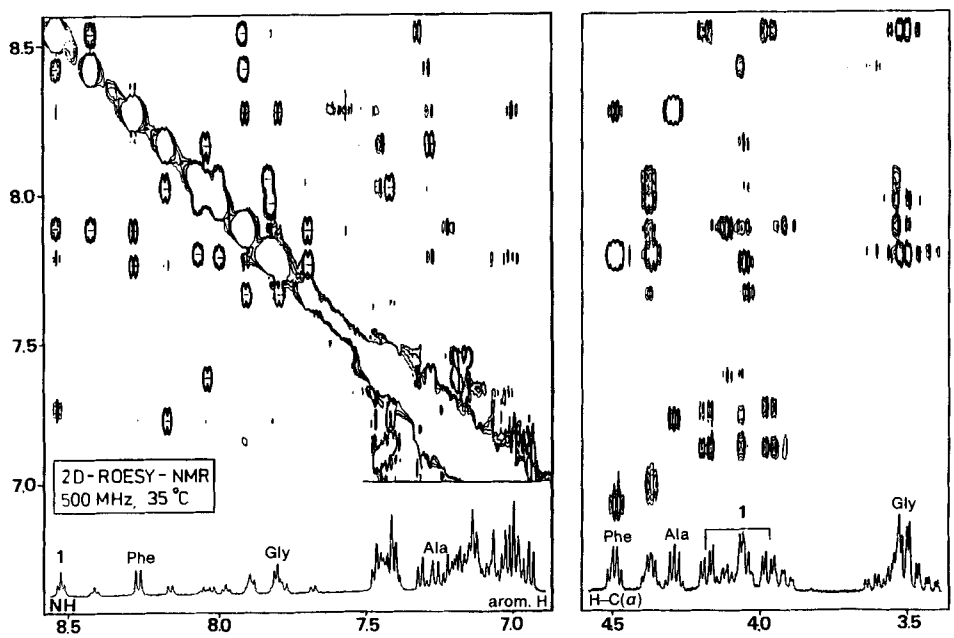


Fig. 3. *Expanded parts of a 500-MHz 2D-ROESY spectrum of* **5** *in* ($D_6$)*DMSO at 35°* (mixing time 200 ms). The NH/NH (left) and the NH/H–C(α) expansion (right) is shown. Positive and negative contours (marked with a minus sign) are drawn at identical levels. The NH/NH expansion (left part) contains many negative cross-peaks due to chemical exchange (the diagonal signals are also negative).

define the dihedral angles ($\phi$ in the peptide part), NOESY (or ROESY) spectra determine qualitatively nuclear distances, and the temperature-dependence of the chemical shift of the NH's indicates H-bonding. The results are compiled in *Table 1*. The $^3J$(NH,H–C($\alpha$))'s of **5** and **6** (major form of $C_2$ symmetry) are in good agreement with extended peptide chains with $\phi = 150°$, as it is expected for a $\beta$-sheet [11]. Conformational averaging is probably present at the Gly residue, and the orientation of the $CH_2N$ group of the unit **1** is unknown (see below). The coupling constants are of course only indicators for the proposed conformation in solution, specially at values close to 7.5 Hz, which are also expected in peptides where free averaging around $\phi$ takes place [12]. Additional support for an extended conformation for the major $C_2$ form of **5** comes from NOE data (see 2D-ROESY [13] spectrum of **5** in *Fig. 3*). Strong cross-peaks connecting the NH's of Phe, Gly, and the biphenyl unit **1** with H–C($\alpha$) of the preceding residue (see also *Exper. Part*) indicate a *cis*-orientation of these protons ($\psi$-values of *ca.* 150°). Weak cross-peaks between the NH's and the H–C($\alpha$) of the same amino acid can be explained by *trans*-orientation of these protons ($\phi = 150°$). The data support an extended conformation. The 2D-ROESY spectrum of **6** gives a similar picture.

Two different patterns of H-bonding are possible in extended conformations of compounds **5** and **6** (see *Fig. 4*): the first pattern gives rise to conformation **C** which is analogous to that of **4** in the solid state (*e.g.* H-bonds between NH(Abc) and CO(Abc)). The second pattern is realized in conformation **D** in which the planes of all amide bonds are rotated by 180° (the spacer **1** replaces here the two central amino acids of a $\beta$-turn).

Table 1. *Vicinal Coupling Constants* $^3J(NH,H-C(\alpha))$ [Hz], *Derived Dihedral Angles* $\phi$, *and Temperature Dependence of the Chemical Shift of the Amide Protons* $d\delta(NH)/dT$ [–ppm/K · $10^3$] *in the Dominant* $C_2$ *Form of* **5** *and* **6** *in* $(D_6)DMSO$

| | | Ala | Phe | Gly | Abc(**1**) |
|---|---|---|---|---|---|
| **5** | $^3J$(NH,H–C($\alpha$)) | 8.5 | 8.2 | 4.8, 5.5 | 5.9, 6.2 |
| | $\phi$[a]) | 0–18, 144–152 | 0–22, 142–150 | 36–44, 30–38; 123–130, 128–136 | 26–39, 129–142 |
| | $d\delta(NH)/dT$ | 2.8 | 6.0 | 3.7 | 6.3 |
| | | Ala | Val | Gly | Abc(**1**) |
| **6** | $^3J$(NH,H–C($\alpha$)) | 8.3 | 9.0 | 6.1, 3.2 | 6.0, 6.0 |
| | $\phi$[a]) | 0–22, 143–151 | 0–15, 147–156 | 27–37, 49–55; 130–138, 113–120 | 28–38, 130–137 |
| | $d\delta(NH)/dT$ | 2.6 | 6.0 | 3.7 | 6.3 |
| | | Ala | Val | Gly | Abc(**1**) |
| Values expected in a $\beta$-sheet | $^3J$(NH,H–C($\alpha$)) | 8.5 | 8.5 | 8.5, 0.0[b]) | –[c]) |
| | $\phi$[b]) | 150 | 150 | 150, 90[b]) | –[c]) |
| | $d\delta(NH)/dT$ | < 3 | > 6 | < 3 | > 6 |

[a]) The *Bystrov-Karplus* equation [17] is used for the estimation of the torsional angles. Two values are noted for $\phi$ due to the form of the *Karplus* curve. The large angle can be compared to the dihedral angle expected for a $\beta$-sheet.

[b]) These values are predicted for a static $\beta$-sheet; conformational averaging at the Gly residue is probably present (see below).

[c]) The orientation of the $CH_2$ group in **1** is unknown without detailed calculations (see below).

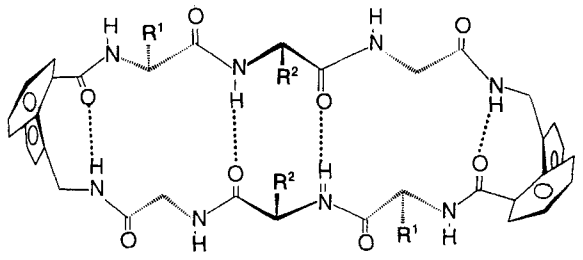

C

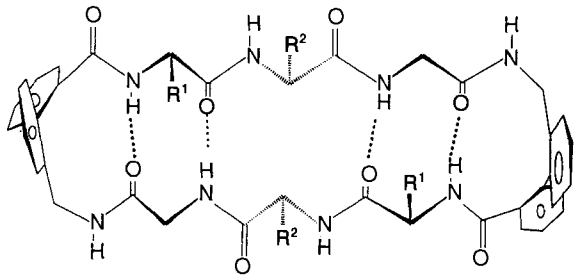

D

Fig. 4. *Schematically drawn β-sheet forms* **C** *and* **D** *of* **5** *and* **6** *with different H-bonding patterns*

Four H-bonds are present in both **C** and **D**, and two types of NH's are involved in these bonds which can eventually be discriminated by the temperature dependence of their chemical shift. Indeed, relatively small $T$-gradients were found for the NH's of Ala and Gly in the dominant form of **5** and **6** (*Table 1*), indicating their involvement in H-bonding. Conformation **D** is compatible with the data of **5** and **6** (*Table 1*), but not with **C**.

A remarkable observation in the $^1$H-NMR spectra of both **5** and **6** is the chemical shift of 2 of the 4 Me(Ala) signals at unusually high field (0.34 and 0.50 ppm; see *Fig. 2*; usually, Me(Ala) signal at 1.0 ppm). One of these signals belongs to the dominating isomer of $C_2$ symmetry, the other is due to 1 Me group of the $C_1$ isomer. The anisotropy of the Ph ring of Phe in **5** is probably not the reason for the unusual chemical shift, because similar high-field signals are also observed for **6** which does not contain Phe. Modelling and molecular-dynamics studies indicate that the relative position of Ala and one of the biphenyl rings explains the unusual chemical shifts (see below).

*Compounds* **7** *and* **8** *Containing the Biphenyl Bridge* **2**. It was not possible yet to isolate one atropisomer of **7** or **8**, neither by crystallization nor by chromatography. $^1$H-NMR Spectra ((D$_6$)DMSO) show four sets of signals of approximately equal intensity, so the three possible diastereoisomers **7** and **8** are in the statistical distribution. The correct assignment of the individual signals of each diastereoisomer is very difficult. COSY Spectra give some useful information. *E.g.*, the expected 16 cross-signals for the NH/H–C($\alpha$) correlations in the diastereoisomer mixture **7** are resolved in 4 groups in the COSY spectrum. The NH(Phe) and NH(Aba) (of group 1 and 2) are located at low field (8.55–8.25 ppm) and the NH(Ala) and NH(Gly) (group 3 and 4) at higher field (8.20–7.90 ppm). The NH's of one type of amino acid have similar chemical shifts in all three

diastereoisomers (variance in $\delta < 0.3$ ppm). The H–C($\alpha$)'s are also arranged in groups depending on the type of the amino acid. This indicates a similar conformational behavior of the peptide part of the 3 diastereoisomers, but more definitive conclusions cannot be drawn. The data of ROESY spectra agree with extended conformations (strong cross-peaks between NH of one residue and H–C($\alpha$) of the preceding residue, weak cross-peaks between NH and H–C($\alpha$) of the same residue). However, the complexity of the spectra does not allow to extract more detailed informations, for example the vicinal coupling constants ($^3J$(NH,H–C($\alpha$)).

**Molecular-Dynamics (MD) Calculations for Peptide Analog 5.** – The most convincing experimental conclusions were derived so far for compound **5** in solution (see above): all NMR data support a $\beta$-sheet structure as in form **D** (see *Fig. 4*) for the more strongly populated atropisomer of **5** having $C_2$ symmetry.

A molecular-dynamics study was performed to get a survey of the conformational space that can be reached by compound **5** and to answer the following questions: *1*) Is the proposed $\beta$-sheet conformation **D** stable in a molecular-dynamics simulation at 300 K? *2*) What are the predicted energetic and geometric differences between the two classes of conformations with (*R*,*R*)- and (*S*,*S*)-chirality of the biphenyl groups? *3*) Is it possible to locate the global minimum on the energy surface? We used the GROMOS-program package [14] for the MD calculations. The program is well parametrized for peptides (and nucleic acids), but minor modifications of the parameter sets had to be made in this study to give a reasonable description of the biphenyl units as far as this is possible with a united-atom force field (see *Exper. Part*).

Initial MD simulations of **5** at 300 K reached only a few energetically accessible conformations within a simulation period of 200 ps. A further extension of the simulation time seemed unjustified, since, when starting with arbitrarily chosen extended geometries of the appropriate biphenyl chirality, considerable changes of the conformation were observed only during the first few ps of the simulation. Especially the H-bonding pattern remained constant. Obviously, energetically favored conformations of **5** were found, but the rate of interconversion to other possible forms was too slow to be followed by the limited simulation time of MD calculations.

However, MD calculations at high temperatures give access to a more complete area of the conformational space [15]. Therefore, arbitrarily chosen extended starting geometries of **5** ((*R*,*R*)- and (*S*,*S*)-class) were used for 20-ps MD calculations at 800 K. The coordinates were sampled at each 0.2 ps of this calculation which resulted in a total of 100 × 2 new geometries. Each of these geometries was first energetically minimized and than further relaxed in 20-ps MD runs at 300 K. The biphenyl chirality did not change within the entire procedure. The obtained 2 × 100 final conformations were minimized again with the force field to give energies and geometries which may provide a more complete picture of the favored conformations of **5**. *Fig. 5* gives a graphical impression of how many stable conformations were found within an energy range of *ca.* 10 kcal/mol.

The (*R*,*R*)-class of conformations of **5** is calculated to be more stable than the (*S*,*S*)-class by 7 kcal/mol. The experimental data also support a dominant form of $C_2$ symmetry in solution, but the energy difference to the second $C_2$ form is probably less than 2 kcal/mol, provided the entropy of the different diastereoisomers is approximately equal. The global minimum found in the calculations is a $\beta$-sheet form of (*R*,*R*)-configuration, $\beta$1. This extended form has all conformational elements which were so far derived qualitatively from the NMR data of the major $C_2$ form of **5** in solution (see above), although the solvent was not included in the calculations. The structure is given in *Fig. 6*, together with three other forms of low energy. *Fig. 7* shows the occurrence of H-bonds in a MD run of 200 ps at 300 K when the $\beta$-sheet form of lowest energy ($\beta$1, (*R*,*R*)) is used as the starting geometry. As expected, the basic H-bonding pattern does not change within 200 ps.

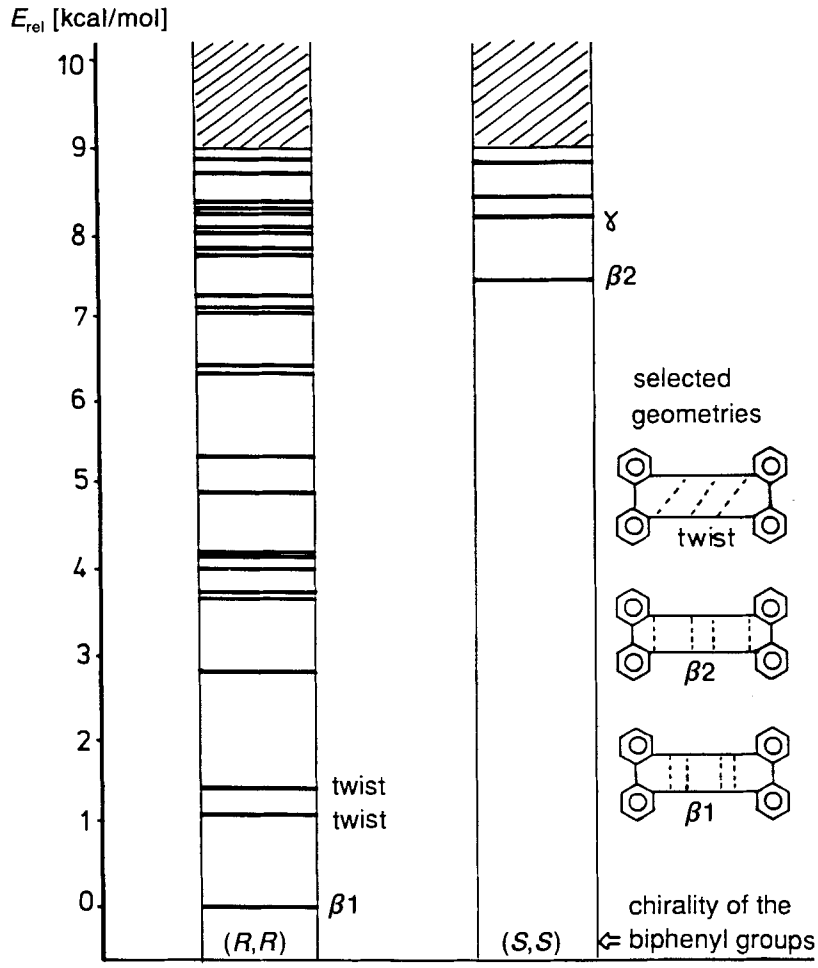


Fig. 5. *Calculated relative energies* (GROMOS force field) *for different conformations of* **5** *with* (R,R)- *and* (S,S)-*chirality of the biphenyl groups.* The conformations are generated with a quenched high-temperature MD technique (see text).

Considering the qualitative agreement of the global minimum of the calculations suggesting the β-sheet form β1 ((*R*,*R*)-class see *Fig. 6*) with the $^1$H-NMR data suggesting conformation **D** (see *Table 1* and *Fig. 4*) for the major form of **5**, the MD simulation of this form at 300 K can serve to explain in more detail some experimental observations: *a*) the measured $^3J$ for the NH–CH moieties which deviate at the Gly and biphenyl residue from the values expected for an ideal β-sheet, *b*) the chemical shift of the Me group of Ala at high field, and *c*) a more quantitative distance correlation with the ROESY data.

*Table 2* compares the time-averaged $^3J$(NH,H–C(α)) of a 300-K 200-ps MD simulation of the β1 form of **5** (*Fig. 6*) to the experimental data. The agreement is excellent, the averaged *J* values at the Gly and biphenyl residue are well explained. *Fig. 8* visualizes the position of the Me(Ala) group with respect to one of the aromatic rings of the biphenyl

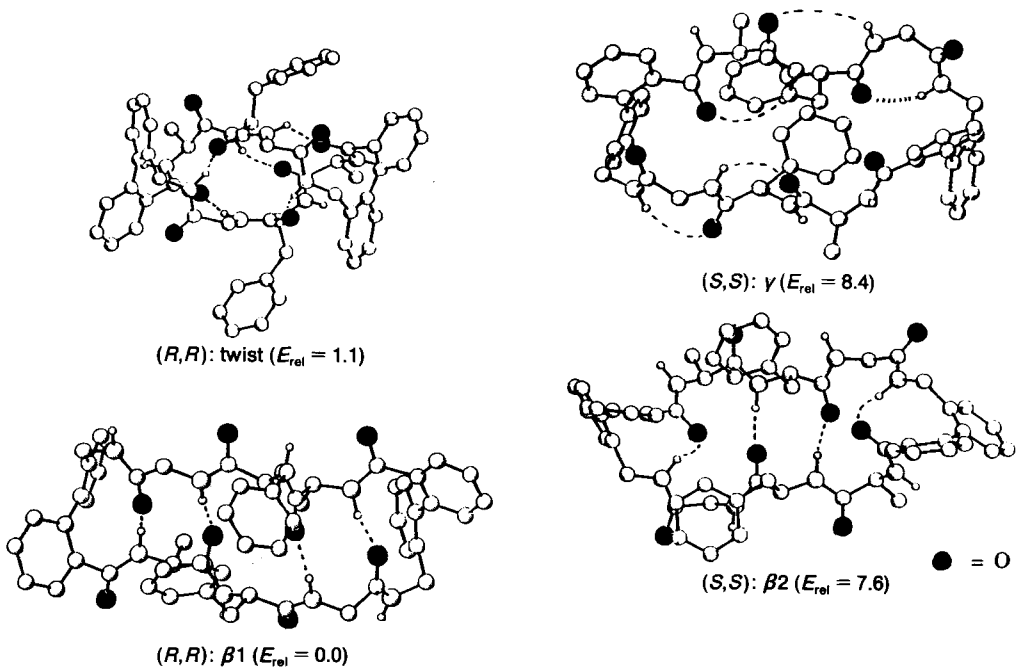


Fig. 6. *Conformations of low energy for* **5**. Relative energy $E_{rel}$ in kcal/mol (see *Fig. 5*). Only NH protons are drawn, all CH protons are omitted.

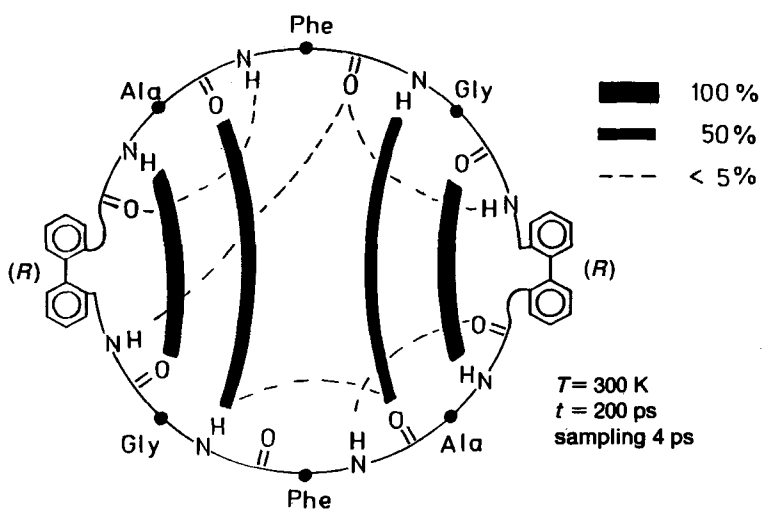


Fig. 7. *Persistency of H-bonds in a 200-ps MD simulation starting with the β1 Form of* **5**. A thick line notes that a large percentage of the structures contains that H-bond during the simulation time.

Fig. 8. *Position of the Me group of Ala over an aromatic ring of the biphenyl group in a MD calculation of* **5** (form $\beta 1$ of (*R,R*)-chirality, 300 K, 200 ps). The points represent the centroid of the Me protons. The distance to the plane of the aromatic ring varies between 3.2 and 4.7 Å, so the Me group is never 'side-on-coordinated'.

Table 2. *Experimental Coupling Constants* $^3J(NH,H-C(\alpha))$ [Hz] *and Corresponding Averaged Values of the Dominant Atropisomer of* **5** *Calculated from a Molecular-Dynamics Simulation of the β-Sheet Form β1 of* **5** ((*R,R*)-chirality, 300 K, 200 ps)

| | Residue in **5** | | | |
|---|---|---|---|---|
| | **1** | Ala | Phe | Gly |
| $^3J$(NH,H–C(α)) (exper.) | 5.9, 6.2 | 8.5 | 8.2 | 4.8, 5.5 |
| $^3J$(NH,H–C(α)) (calc.) | 6.0, 6.2 | 8.7 | 8.9 | 5.2, 6.1 |
| Fluctuation in $\phi$ (r.m.s.) | 15° | 13° | 11° | 49° |

unit in the same simulation. Obviously, a conformation is maintained which positions Me(Ala) in the shielding region of one benzene ring explaining the observed high-field shift. Similar calculations starting with the (*S,S*)-form of lowest energy ($\beta 2$ in *Fig. 6*) do not produce that proximity. Consequently, we assume that the major form of $C_2$ symmetry of **5** whose Me(Ala) groups are located at high field has both biphenyl groups in (*R*)-configuration.

Finally, *Table 3* correlates the averaged distances of the 300-K MD simulation of the (*R,R*)-isomer ($\beta 1$) with distances derived from the cross-peak volumina of the 2D-ROESY spectra (for details, see *Exper. Part*). The correlation is surprisingly good for such an error-prone method [16]. Again the $\beta$-sheet form of (*R,R*)-chirality, $\beta 1$, explains the $^1$H-NMR data well.

**Conclusions.** – The $^1$H-NMR data for the major solution form of the compounds **5** and **6** containing the 'short' biphenyl bridge **1** are consistent with an extended peptide conformation as in a $\beta$-sheet. The chemical shift of the Me(Ala) groups is best explained by the (*R*)-configuration of both biphenyl groups. The H-bonding pattern of the major form in ($D_6$)DMSO solution is in accord with conformation **D** (*Fig. 4*), and the NOE distances support a similar conformation, $\beta 1$ in *Fig. 6*. This is in contrast to the conformation observed in the X-ray structure of the previously reported cyclopeptide **4** which contains only one amino acid in the peptide chains separating the two biphenyl moieties: an inverted H-bonding pattern comparable to form **C** (*Fig. 4*) is found in the solid state as

Table 3. *Comparison of Nuclear Distances* $r_{ij}$ [Å] *between Protons NH, CH, and Me Estimated from ROESY Experiments with Distances Calculated for the β-Sheet Form of* **5**[a])

| Proton pair $i/j$[b]) | $s_{ij}\cdot 10^2$[c]) | $s_{ji}\cdot 10^2$[c]) | $r_{ij}$(NOE)[d]) | $r_{ij}(\beta 1)$[d]) |
|---|---|---|---|---|
| NH(Abc)/NH(Phe) | [e]) | [e]) | – | > 4.5 |
| NH(Abc)/NH(Gly) | 0.91 | [f]) | 3.64 | 4.25 |
| NH(Abc)/NH(Ala) | [e]) | [e]) | – | > 4.5 |
| NH(Abc)/(H–C(2)(Phe) | [e]) | [e]) | – | > 4.5 |
| NH(Abc)/H–C(2)(Ala) | [e]) | [e]) | – | > 4.5 |
| NH(Abc)/$CH_a$–C(2′)(Abc) | 2.77 | 4.27 | 2.90 | 2.71 |
| NH(Abc)/$CH_b$–C(2′)(Abc) | 3.92 | 6.38 | 2.73 | 2.24 |
| NH(Abc)/$H_a$–C(2)(Gly) | 3.11 | 8.35[g]) | 2.71[g]) | 2.12 |
| NH(Abc)/$H_b$–C(2)(Gly) | 3.01 | 8.35[g]) | 2.71[g]) | 3.04 |
| NH(Abc)/$CH_2$(3)(Phe) | [e]) | [e]) | – | > 4.5 |
| NH(Abc)/Me(Ala) | [c]) | [c]) | – | > 4.5 |
| NH(Phe)/NH(Gly) | [c]) | 0.55 | 4.0 | 4.15 |
| NH(Phe)/NH(Ala) | 1.99 | 0.93 | 3.40 | 4.29 |
| NH(Phe)/H–C(2)(Phe) | 1.94 | [g]) | 3.19 | 2.92 |
| NH(Phe)/H–C(2)(Ala) | 10.23 | 12.48 | 2.38 | 2.33 |
| NH(Phe)/$CH_2$(2′)(Abc) | [e]) | [e]) | – | > 4.5 |
| NH(Phe)/$CH_2$(2)(Gly) | [e]) | [e]) | – | > 4.5 |
| NH(Phe)/$H_a$–C(3)(Phe) | 1.10 | 1.78 | 3.38 | 3.25 |
| NH(Phe)/$H_b$–C(3)(Ph) | 2.69 | 4.55 | 2.90 | 2.67 |
| NH(Phe)/Me(Ala) | 1.00 | 2.51 | 3.31 | 4.18[h]) |
| NH(Gly)/NH(Ala) | 1.95 | 1.20 | 3.34 | 3.63[i]) |
| NH(Gly)/H–C(2)(Phe) | 9.37 | 13.49 | 2.38 | 2.42 |
| NH(Gly)/H–C(2)(Ala) | [c]) | [e]) | – | > 4.5 |
| NH(Gly)/$CH_2$–C(2′)(Abc) | [e]) | [e]) | – | > 4.5 |
| NH(Gly)/$CH_2$(2)(Gly) | [f]) | 7.71[g]) | 2.53 | 2.58[j]) |
| NH(Gly)/$H_a$–C(3)(Phe) | [f]) | 1.22 | 3.44 | 3.80 |
| NH(Gly)/$H_b$–C(3)(Phe) | [f]) | [e]) | – | > 4.5 |
| NH(Gly)/Me(Ala) | 0.59 | 1.40 | 3.51 | 4.50[h]) |
| NH(Ala)/H–C(2)(Phe) | [e]) | [c]) | – | > 4.5 |
| NH(Ala)/H–C(2)(Ala) | 2.36 | 3.18 | 3.01 | 2.90 |
| NH(Ala)/$CH_a$–C(2′)(Abc) | [f]) | 1.37 | 3.38 | 4.21[i]) |
| NH(Ala)/$CH_b$–C(2′)(Abc) | [f]) | 0.92 | 3.61 | 4.90 |
| NH(Ala)/$CH_2$(2)(Gly) | [e]) | [e]) | – | > 4.5 |
| NH(Ala)/$CH_2$(3)(Ph) | [e]) | [e]) | – | > 4.5 |
| NH(Ala)/Me(Ala) | 5.14 | 3.26 | 2.83 | 3.17[h]) |

[a]) The $\beta 1$ form with (*R*,*R*)-biphenyl chirality is used as reference, see text and *Fig. 6*.

[b]) The proton pairs are listed according to their chemical shifts. The subscripts a and b refer to diastereoisotopic geminal protons.

[c]) The abreviations $s_{ij}$ and $s_{ji}$ stand for the volume ratios of cross to diagonal peaks (compensated for offset effects, see *Exper. Part*).

[d]) The distances $r_{ij}$(NOE) and $r_{ij}(\beta 1)$ are derived from the NOE data or calculated from the averaged $\beta 1$ form, respectively.

[e]) Cross-peaks with (compensated) intensities < 0.5% are not evaluated.

[f]) Only one $s_{ij}$ is reliable.

[g]) The geminal protons are not resolved in the $f2$ dimension.

[h]) Distance to the centroid of the Me protons.

[i]) Interchain distance.

[j]) Closest distance.

well as in solutions of **4** [4]. However, the X-ray structure of **4** shows biphenyl groups of (*S*)-chirality. Consequently, we postulate that the H-pattern induced by pseudo-amino acid **1** depends on the chirality of the biphenyl groups (see **E** and **F**).

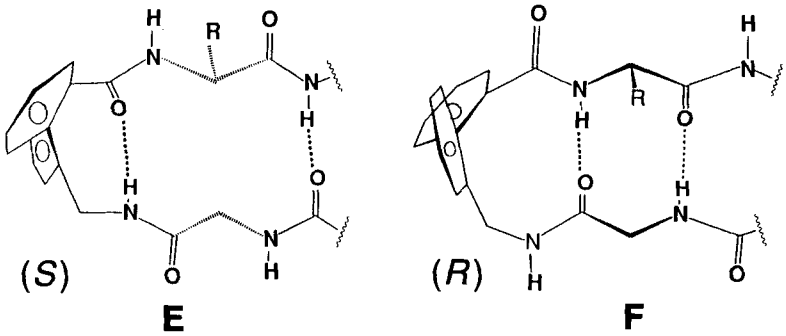


**E** **F**

The data discussed in this paper may serve as a guide for the design of synthetic biphenyl compounds with peptide conformations fixed in a $\beta$-sheet arrangement. However, complications arise from the fact that atropisomers interconvert relatively fast and cannot be isolated. Therefore, the structural analysis has to deal with mixtures. This limits the general value of the unit **1** as model system. More rigid substituted biphenyls or the binaphthyl group may be better suited for the proposed stereochemical induction and are currently incorporated into cyclopeptides.

## Experimental Part

*General.* The tripeptides Boc-Ala-Phe-Gly-OMe, Boc-Gly-Phe-Ala-OMe, and Boc-Ala-Val-Gly-OMe were prepared by classical peptide methods [8–10] from L-amino acids (*Fluka* or *Degussa*). M.p.: uncorrected. $^1$H-NMR Spectra (synthetic part): *Jeol-JNM-GX400* (400 MHz) instrument; $\delta$ in ppm rel. to $Me_4Si$. DCI (direct chemical ionisation)-MS: *MAT-8222* spectrometer; in *m/z* (rel. %).

*2D NMR Studies and Distance Calculations.* COSY, ROESY, and TOCSY $^1$H-NMR Spectra: at 400 MHz on a *Jeol-GX400* instrument for signal assignments. The 500-MHz-ROESY (*Fig. 3*) serves as the basis of the distance evaluation; it was obtained with a 500-MHz-*Varian-UNITY* system on a degassed sample of **5** (5 mg in 0.4 ml of $(D_6)$DMSO) at 35°. The following measuring parameters were used: Cw-spinlock puls sequence with a lock field of 2.5 kHz strength centered at 4.6 ppm; mixing time 200 ms; spectral width 5 kHz; 4K $f2$ points, 400 $f1$ transients (16 scans each).

The 2D-matrix was transferred to an *Iris-INDIGO* workstation and processed with the FELIX 2.0 software [18]. An exponential window function ($lb$ = 0.73 Hz) was used in $f2$; $f1$ was multiplied by a sine-square function shifted by 90 deg (zero filling to 2 K). The first 2 data points in $f1$ were constructed by linear prediction.

The ratios $s_{ij}$ ( $= I_{ij}/I_{ii}$) of cross- to diagonal-peak volume integrals were divided by $\sin^2\alpha_j$ to correct for off-resonance effects according to [19] ($\alpha_j$ is the off-resonance angle of spin $j$ to the lock field). The corrected ratios $s_{ij}$ were finally used to obtain distances $r_{ij}$ by calibration with the distance $r(H\text{–}C(2)(Ala)/Me(Ala))$ (2.5 Å; centroid of Me) according to $r_{ij}/r(H\text{–}C(2)/(Ala)/Me(Ala) = (s(H\text{–}C)(2)(Ala)/Me(Ala)/s_{ij})^{1/6}$. The distances $r_{ij}$ (NOE) in *Table 3* are averaged over $r_{ij}$ and $r_{ji}$ if the volume integrals of both cross-peaks are accessible. The correlation of the derived distances $r_{ij}$ (NOE) with distances $r_{ij}$ ($\beta1$) calculated by MD techniques is relatively good (see *Table 3*), despite the fact that the method described above has severe limitations (isolated spin pair approximation, uniform correlation time, neglect of scalar coupling, referencing to only one 'virtual' distance). 400-MHz-ROESY Spectra with shorter mixing times (50 and 100 ms) do not improve the correlation, but noise and $J$-artefacts are significantly enhanced.

Further complications arise from the presence of chemical exchange in **5** (see *Fig. 3*). However, the intensity ratio $s_{ij}$ (negative) of the exchange cross-peaks accounts only to $4\cdot10^{-2}$ at 35°. If a strong NOE ($s_{ij} = 10\cdot10^{-2}$) in one of the minor isomers is transferred by chemical exchange to the signals of the investigated major isomer, this

will lead only to a false signal of an intensity less than $0.4 \cdot 10^{-2}$, outside the limit ($0.5 \cdot 10^{-2}$) used in *Table 3*. Distortions due to chemical exchange are certainly present, but the distance correlation in *Table 3* should not be affected significantly.

*MD Calculations.* The GROMOS package [14] with the force field IFP37C4 was used for the MD simulations of **5**. Initial calculations show that 1,4-repulsions at the biphenyl bond (between the atoms C(2), C(2′) and C(6), C(6′)) result in an out-of-plane bending of the benzene rings. Therefore, the force constants for the improper dihedrals at the positions C(1), C(1′), C(2), C(2′), and C(3), C(3′) were increased from 40 to 200 kcal/rad. In addition, the force constant for the improper dihedral angle of the type 27 ($C_B$–X–Y–$C_{R61}$) was increased to 80 kcal/rad.

Initial velocities for the MD simulations at 800 and 300 K were taken from the *Maxwell* distribution. Weak coupling to the temp. bath with 0.1 ps couplings constant and a temp. tolerance of 10 K kept the temp. constant. The time step of the simulation was 2 fs, and coordinates were sampled each 0.1 (or 0.2) ps. All calculations were done without constraints.

Averaged N*H*–C*H* coupling constants were obtained with the program AJC in the GROMOS package (MD simulation of the $\beta$1-form of **5** at 300 K, *Table 2*). The equation $J = 6.4 \cos^2 \alpha - 1.4 \cos \alpha + 1.9$ was used as the anal. form of the *Karplus* equation [20].

*2′-{[(*tert*-Butyloxy)carbonyl]aminomethyl}biphenyl-2-carboxylic Acid* (*Boc-Abc*; **9**). A soln. of 2′-(phthalimidomethyl)-biphenyl-2-carboxylic acid [5] (30 mmol) in MeOH/$NH_2NH_2 \cdot H_2O$ 10:1 (110 ml) was heated to 50° for 5 h. A precipitate (phthalohydrazide) was filtered off and the filtrate evaporated. Then, KOH (1.7 g) in $H_2O$ (50 ml) was added, followed by a soln. of di(*tert*-butyl) dicarbonate (6.6 g, 30 mmol) in dioxane (50 ml). The mixture was stirred 3 days at 25°. The soln. was concentrated to 50 ml and cooled to 0° $Et_2O$ (50 ml) added, and the mixture acidified to methyl red with HCl. After phase separation, the aq. layer was extracted again with $Et_2O$ (50 ml). The combined org. layers were dried ($MgSO_4$) and evaporated. Recrystallization of the crude product from $CH_2Cl_2$/petroleum ether yields 3.3 g (34%) of a colorless solid. M.p. 129–132°. $^1$H-NMR ($CDCl_3$): 11.0 (*s*, COOH); 8.15 (*d*, 1 arom. H); 8.7–7.9 (*m*, 7 arom. H); 5.1 (br., NH); 4.18 (*AB*, $CH_2$); 1.48 (*s*, *t*-Bu). Anal. calc. for $C_{19}H_{21}NO_4$: C 69.72, H 6.42, N 4.28; found: C 69.56, H 6.52, N 4.35.

*2′-{[(*tert*-Butyloxy)carbonyl]aminomethyl}biphenyl-2-acetic Acid* (*Boc-Aba*; **10**). As described for **9**, with 2′-(phthalimidomethyl)biphenyl-2-acetic acid [5] as starting material. Evaporation of the $Et_2O$ layers yielded 6.8 g (67%) of an oily material, which was used without purification in the next transformations. $^1$H-NMR ($CDCl_3$): 8.85–8.55 (1H,COOH); 7.40–7.00 (*m*, 8 arom. H); 5.72 (br., NH); 4.76 (br., NH); 3.94 (*AB*, br., $CH_2N$); 3.27 (*AB*, $CH_2CO$); 1.30 (*s*, *t*-Bu). EI-MS: 341 (2, $M^+$), 285 (76), 284 (72), 267 (21), 180 (100). The dicyclohexylammonium salt was used for an elemental analysis: Anal. calc. for $C_{32}H_{46}N_2O_4 \cdot \frac{1}{2} H_2O$: C 72.32, H 8.85, N 5.27; found: C 72.12, H 8.82, N 5.43.

*General Procedure I: Peptide Coupling* [7]. To a precooled soln. (−10°) of the carboxyl component (10 mmol) and of the amino component (10 mmol) in dry $CH_2Cl_2$ (100 ml) *N*-methylmorpholine (NMM; 6.0 ml) was added. After addition of propylphosphonic anhydride (PPA; 50% in $CH_2Cl_2$; 8.0 ml), the mixture was stirred at r.t. for 2 days. The solvent was evaporated and the residue taken up in AcOEt (100 ml). The soln. was washed with sat. $NaHCO_3$ soln., $NaHSO_4$ soln. (5%), and brine, dried ($MgSO_4$), and evaporated, and the residue was recrystallized.

*Methyl {2′-{[(*tert*-Butyloxy)carbonyl]aminomethyl}biphenyl-2-carbonyl}-*L*-alanyl-*L*-phenylalanyl-glycinate* (*Boc-Abc-Ala-Phe-Gly-OMe*; **11**) was prepared according to the *General Procedure I* from **9** (10 mmol) and H-Ala-Phe-Gly-OMe. Evaporation of the AcOEt soln. gave **11** as slightly yellow solid (2.75 g, 44%) which was used in the next steps without further purification and analysis.

*Methyl {2′-{[(*tert*-Butyloxy)carbonyl]aminomethyl}biphenyl-2-carbonyl}-*L*-alanyl-*L*-valyl-glycinate* (*Boc-Abc-Ala-Val-Gly-OMe*; **12**). Preparation according to the *General Procedure I* and recrystallization from AcOEt gave **12** as a white solid (1.8 g, 31%). M.p. 194–197°. $^1$H-NMR ($CDCl_3$): two sets of signals of similar intensity (atropisomerism of the biphenyl groups); 7.76–6.65 (*m*, 21 H, arom. H, NH); 6.32 (*d*, 1 H, NH); 5.50 (*t*, 1 H, NH(Abc)); 5.40 (*t*, 1 H, NH(Abc)); 4.30–3.94 (*m*, 12 H, H–C(α)'s, $CH_2$(Abc)); 3.68 (*s*, 3 H, MeO); 3.65 (*s*, 3 H, MeO); 2.10 (*m*, 2 H, H–C(3)(Val)); 1.29 (*s*, 9 H, *t*-Bu); 1.00 (*d*, 3 H, Me(Ala)); 0.83 (*m*, 12 H, Me(Val)); 0.71 (*d*, 3 H, Me(Ala)). EI-MS: 568 (87, $M^+$), 513 (28), 450 (88), 438 (60), 381 (100), 325 (89), 324 (95). Anal. calc. for $C_{30}H_{40}N_4O_7$: C 63.38, H 7.04, N 9.86; found: C 63.03, H 6.95, N 9.77.

*Methyl {2′-{[(*tert*-Butyloxy)carbonyl]aminomethyl}biphenyl-2-acetyl}-glycyl-*L*-phenylalanyl-*L*-alaninate* (*Boc-Aba-Gly-Phe-Ala-OMe*; **13**) was prepared by *General Procedure I*. Recrystallization from acetone gave **13** as a colorless solid (1.3 g, 57%). M.p. 141–145°. $^1$H-NMR ($CDCl_3$, 23°): no splitting observed at 400 MHz; 7.45–7.07 (13 arom. H); 6.73 (br., NH); 6.51 (br., NH); 6.44 (br., NH); 5.15 (*t*, NH); 4.60 (*q*, H–C(2)(Phe)); 4.45 (*m*, H–C(2)(Ala)); 3.99 (*AB*, $CH_2N$(Aba)); 3.80–3.60 (*AB*, $CH_2$(2)(Gly)); 3.70 (*s*, MeO); 3.35 (*AB*, $CH_2CO$(Aba));

3.12–2.91 (*m*, $CH_2$(3)(Phe)); 1.36 (*s*, *t*-Bu); 1.29 (*d*, Me(Ala)). Anal. calc. for $C_{35}H_{42}N_4O_7 \cdot H_2O$: C 64.80, H 6.83, N 8.64; found: C 64.49, H 6.70, N 8.90.

*Methyl {2'-{[(tert-Butyloxy)carbonyl]aminomethyl}biphenyl-2-acetyl}-L-alanyl-L-phenylalanyl-glycinate* (*Boc-Aba-Ala-Phe-Gly-OMe*; **14**). Preparation according to *General Procedure I* and recrystallization from AcOEt/petroleum ether gave **14** as a white solid (3.1 g, 49%). $CHCl_3$ solns. of **14** contained both possible diastereoisomers ((*R*)- or (*S*)-biphenyl chirality) in equal amounts. $^1$H-NMR ($CDCl_3$, 23°): most signals split; 7.45–7.05 (26 H, arom. H, NH); 6.82 (br., 2 H, NH); 6.68 (*d*, 1 H, NH); 6.46 (br., 2 H, NH); 6.40 (br., 1 H, NH); 5.22 (*t*, 1 H, NH); 5.16 (br., 1 H, NH); 4.65 (*m*, 2 H, H–C(2) (Phe)); 4.25 (*m*, 1 H, H–C(2)(Ala)); 4.10–3.80 (*m*, 9 H, 2 $CH_2$N(Aba), 2 $CH_2$(2)(Gly), H–C(2)(Ala)); 3.71 (*s*, 3 H, MeO); 3.69 (*s*, 3 H, MeO); 3.47–2.95 (*m*, 8 H, 2 $CH_2$CO(Aba), 2 $CH_2$(3)(Phe)); 1.39 (*s*, 9 H, *t*-Bu); 1.37 (*s*, 9 H, *t*-Bu); 1.18 (*d*, 3 H, Me(Ala)); 1.09 (*d*, 3 H, Me(Ala)). Anal. calc. for $C_{35}H_{42}N_4O_7 \cdot \frac{1}{2} H_2O$: C 65.71, H 6.77, N 8.76; found: C 65.83, H 6.63, N 8.75.

*Linear Precursors to the Cyclization: Compounds* **15–18**. The products **11–14** were divided in two equal portions: in one portion, the Boc group was removed with dioxane/2N HCl, in the other the ester was saponified with 1N NaOH [8]. The resulting materials were used in a fragment condensation without further characterization and purification.

The C- respectively N-deprotected products from **11–14** were condensed with NMM/PPA according to the *General Procedure I* (see above). The $^1$H-NMR spectra of the resulting linear octapeptides were, as expected, rather complex and at 400 MHz not resolved (*e.g.*, 32 different NH's should exist in one of the linear peptides if all possible combinations of the biaryl chirality were realized). One compound of each type (**16** and **18**) was checked by elemental analysis; all were used in the cyclization steps without further characterization.

*Boc-Abc-Ala-Phe-Gly-Abc-Ala-Phe-Gly-OMe* (**15**): Boc-Abc-Ala-Phe-Gly-OH (1.19 g, 2 mmol) and H-Abc-Ala-Phe-Gly-OMe·HCl (1.08 g, 2 mmol; obtained from **11** as described above) were condensed in $CH_2Cl_2$ (20 ml) with NMM (0.8 ml) and PPA (0.9 ml). The obtained material (1.32 g, 62%) was used directly in the cyclization to **5**.

*Boc-Abc-Ala-Val-Gly-Abc-Ala-Val-Gly-OMe* (**16**): Boc-Abc-Ala-Val-Gly-OH (730 mg) and H-Abc-Ala-Val-Gly-OMe·HCl (665 mg; obtained from **12** as described above) were coupled with NMM (0.8 ml) and PPA (1.5 ml) in $CH_2Cl_2$ (20 ml). Recrystallization from AcOEt yielded **16** (540 mg, 41%). M.p. 164–168°. Anal. calc. for $C_{54}H_{68}N_8O_{11} \cdot$ AcOEt $\cdot \frac{1}{2} H_2O$: C 63.23, H 7.00, N 10.25; found: C 62.96, H 7.01, N 10.45.

*Boc-Aba-Gly-Phe-Ala-Aba-Gly-Phe-Ala-OMe* (**17**): Boc-Aba-Gly-Phe-Ala-OH (500 mg) and H-Aba-Gly-Phe-Ala-OMe·HCl (520 mg; obtained from **13** as described above) were coupled with NMM (0.55 ml) and PPA (1.0 ml) in $CH_2Cl_2$ (20 ml). Recrystallization from acetone yielded **17** (570 mg, 62%).

*Boc-Aba-Ala-Phe-Gly-Aba-Ala-Phe-Gly-OMe* (**18**): Boc-Aba-Ala-Phe-Gly-OH (1.50 g, 2.5 mmol) and H-Aba-Ala-Phe-Gly-OMe·HCl (1.45 g; obtained from **14** as described above) were coupled with NMM (1.6 ml) and PPA (2.0 ml) in $CH_2Cl_2$ (20 ml). Recrystallization from AcOEt gave **18** (970 mg, 35%). Anal. calc. for $C_{64}H_{72}N_8O_{11} \cdot H_2O$: C 67.00, H 6.50, N 9.78; found: C 67.24, H 6.38, N 9.78.

*General Procedure II. Cyclization of* **15–18** *to* **5–8**. A soln. of each **15–18** in MeOH (10 ml) and $NH_2NH_2 \cdot H_2O$ (1.0 ml) was stirred for 15 h. The solvent and excess $NH_2NH_2 \cdot H_2O$ were evaporated. After addition of 2N HCl dioxane (25 ml) the mixture was stirred for 2 h and then evaporated. The residue was dissolved in DMF, the soln. cooled to −20°, and HCl and $NaNO_2$ were added (for amounts, see below). The mixture was stirred for 45 min, diluted with cold DMF (−10°; for amount, see below), and the calculated amount of NMM (see below) added. The mixture was allowed to warm up to 5° overnight (15–20 h). After stirring 2 days at r.t. and evaporation ( < 50°), the residue was dissolved in AcOEt, washed with $NaHCO_3$ soln., $H_2O$, 5% $NaHSO_4$ soln., and brine. The extract was dried ($MgSO_4$) and evaporated and the residue purified by recrystallization.

*Cyclo(-Abc-Ala-Phe-Gly-)$_2$* (**5**): From **15** (1.32 g, 1.2 mmol), 2N HCl/$NaNO_2$ (1.0 ml, 135 mg) DMF (400 ml), and NMM (2.0 ml), after recrystallization from MeCN: **5** (139 mg, 12%). M.p. (loss of solvent > 190°) > 235° (dec.). NOE (from ROESY of major populated form; see *Fig. 3*; *w* = weak, *s* = strong). NH(Ala)/H–C(2)(Ala) *w*; H–C(2)(Ala)/NH(Phe) *s*; NH(Phe)/H–C(2)(Phe) *w*; H–C(2)(Phe)/NH(Gly) *s*; NH(Gly)/$CH_2$(Gly) *w*; $CH_2$(Gly)/NH(Abc) *s*; NH(Abc)/$CH_a$–C(2')(Abc) *w*; NH(Abc)/$CH_b$–C(2')(Abc) *s*; $CH_b$–C(2')(Abc)/H–C(6)(Abc) *s*; $CH_a$–C(2')(Abc)/H–C(3')(Abc) *s*. DCI-MS ($NH_3$, pos.): 986 (20, $[M + NH_4]^+$), 969 (84, $[M + H]^+$), 951 (19), 711 (19), 600 (32), 502 (100). Anal. calc. for $C_{56}H_{56}N_8O_8 \cdot 2H_2O$: C 66.91, H 6.02, N 11.15; found: C 66.71, H 6.17, N 11.11.

*Cyclo(-Abc-Ala-Val-Gly-)$_2$* (**6**): From **16** (540 mg, 0.53 mmol), 2N HCl/$NaNO_2$ (0.4 ml, 45 mg), DMF (200 ml), and NMM (0.8 ml), after recrystallization from $CHCl_3$: **6** (78 mg, 17%). M.p. 206–209°. DCI-MS ($NH_3$, pos.): 890 (6, $[M + NH_4]^+$), 873 (100, $[M + H]^+$), 855 (6), 454 (3), 419 (12). Anal. calc. for $C_{48}H_{56}N_8O_8 \cdot 2CHCl_3$: C 54.01, H 5.26, N 10.08; found: C 53.19, H 5.58, N 10.25.

*Cyclo(-Aba-Gly-Phe-Ala-)$_2$* (**7**): From **17** (570 mg, 0.50 mmol), 2N HCl/$NaNO_2$ (0.4 ml, 35 mg), DMF (150 ml), and NMM (0.8 ml), after recrystallization from acetone: **7** (15 mg, 3%). M.p. 310° (dec.). DCI-MS ($NH_3$, pos.): 997 (100, $[M + H]^+$), 979 (22), 481 (36).

*Cyclo(Aba-Ala-Phe-Gly)$_2$* (**8**): From **18** (920 mg, 0.86 mmol), 2N HCl/$NaNO_2$(0.7 ml, 70 mg), DMF (150 ml), and NMM (1.8 ml), after recrystallization from acetone: **8** (86 mg, 10%). M.p. 279° (dec.). DCI-MS ($NH_3$, pos.): 1014 (100, $[M + NH_4]^+$), 996 (13, $M^+$), 979 (21), 481 (33). Anal. calc. for $C_{58}H_{60}N_8O_8 \cdot 5H_2O$: C 64.09, H 6.45, N 10.31; found: C 63.53, H 6.48, N 9.59.

We particularly thank Dr. *E. Hoffmann, Varian Assoc.*, Darmstadt, for measuring the 500-MHz ROESY spectra and Prof. Dr. *D. Leibfritz*, Dr. *P. Schulze*, and *I. Erxleben*, University of Bremen, for the DCI-MS. The financial support by the *Deutsche Forschungsgemeinschaft* and the *Fonds der Chemischen Industrie* is gratefully acknowledged. *W. H. B. S.* thanks the *Studienstiftung des Deutschen Volkes* for a grant.

## REFERENCES

[1] D. S. Kemp, P. E. McNamara, *J. Org. Chem.* **1985,** *50,* 5834; U. Nagai, K. Sato, *Tetrahedron Lett.* **1985,** *26,* 647; M. Feigel, *J. Am. Chem. Soc.* **1986,** *108,* 181; K. Sato, U. Nagai, *J. Chem. Soc., Perkin Trans. 1* **1986,** 1231; M. Kahn, S. Wilke, B. Chen, K. Fujita, *J. Am. Chem. Soc.* **1988,** *110,* 1638; M. G. Hinds, N. G. Richards, J. A. Robinson, *J. Chem. Soc., Chem. Commun.* **1988,** 1447; I. L. Karle, R. Kishore, S. Raghotham, P. Balaram, *J. Am. Chem. Soc.* **1988,** *110,* 1958; M. Feigel, *Liebigs Ann. Chem.* **1989,** *459*; D. S. Kemp, B. R. Bowen, C. C. Muendel, *J. Org. Chem.* **1990,** *55,* 4650; G. L. Olson, M. E. Voss, D. E. Hill, M. Kahn, V. S. Madison, C. M. Cook, *J. Am. Chem. Soc.* **1990,** *112,* 323; H. Diaz, J. W. Kelly, *Tetrahedron Lett.* **1991,** *32,* 5725; G. Hölzemann, *Kontakte* **1991,** 3; I. Ernest, J. Kalvoda, G. Rihs, M. Mutter, *Tetrahedron Lett.* **1990,** *31,* 4011; H. Diaz, J. R. Espina, J. W. Kelly, *J. Am. Chem. Soc.* **1992,** *114,* 8316; K. Müller, D. Obrecht, A. Knierzinger, S. Chuck, C. Spiegler, W. Bannwarth, A. Trzeciak, G. Englert, A. M. Labhardt, P. Schönholzer, 'Trends in Medicinal Chemistry', VCH Publishers, New York, 1993, chapt. 33, p. 515; U. Nagai, K. Sato, R. Nakamura, R. Kato, *Tetrahedron* **1993,** *49,* 3547; I. Ernest, J. Kalvoda, C. Siegel, G. Rihs, H. Fritz, M. J. J. Blommers, F. Raschdorf, E. Francotte, M. Mutter, *Helv. Chim. Acta* **1993,** *76,* 1539.

[2] H. Kessler, B. Kutscher, A. Klein, *Liebigs Ann. Chem.* **1986,** 893; P. Vander Elst, D. Gondol, C. Wynants, D. Tourwe, G. van Binst, *Int. J. Pept. Protein Res.* **1987,** *29,* 331; K. Sato, M. Hotta, M. H. Dong, H. Hu, J. P. Taulene, M. Goodmann, U. Nagai, N. Ling, *ibid.* **1991,** *38,* 340; N. J. Skelton, M. M. Harding, R. J. Mortishire-Smith, S. K. Rahman, D. H. Williams, M. J. Rance, J. C. Ruddock, *J. Am. Chem. Soc.* **1991,** *113,* 7522; R. Hirschmann, *Angew. Chem.* **1991,** *103,* 1305; *ibid. Int. Ed.* **1991,** *30,* 1278; D. F. Mierke, P. Schmieder, P. Karuso, H. Kessler, *Helv. Chim. Acta* **1991,** *74,* 1953.

[3] J. S. Richardson, *Adv. Prot. Chem.* **1981,** *34,* 167; J. Priestle, M. G. Grütter, J. L. White, M. G. Vincent, M. Kania, E. Wilson, T. S. Jardetzky, K. Kirschner, J. N. Jansonius, *Proc. Natl. Acad. Sci. U. S. A.* **1987,** *84,* 5690; M. Mutter, E. Altmann, K.-H. Altmann, R. Hersperger, P. Koziej, K. Nebel, G. Tuchscherer, S. Vuilleumier, H.-U. Gremlich, K. Müller, *Helv. Chim. Acta* **1988,** *71,* 835.

[4] V. Brandmeier, M. Feigel, M. Bremer, *Angew. Chem.* **1989,** *101,* 466.

[5] V. Brandmeier, M. Feigel, *Tetrahedron* **1989,** *45,* 1365.

[6] C. Toniolo, *CRC Crit. Rev. Biochem.* **1980,** *9,* 1; G. D. Rose, L. M. Gierasch, J. A. Smith, *Adv. Protein Chem.* **1985,** *37,* 1.

[7] H. J. Kleiner, H. Wissmann, *Angew. Chem.* **1980,** *92,* 129.

[8] E. Wünsch, 'Houben-Weyl', Thieme, Stuttgart, 1974, Vol. XV/1, p. 126.

[9] K. H. Dermer, P. Thamm, P. Stenzel, 'Houben-Weyl', Thieme, Stuttgart, 1974, Vol. XV/1, p. 334.

[10] Y. S. Klausner, M. Bodanszky, *Synthesis* **1974,** 549.

[11] J. N. Scarsdale, C. Van Alsenoy, V. J. Klimkowski, L. Schäfer, F. A. Momany, *J. Am. Chem. Soc.* **1983,** *103,* 3438.

[12] H. Kessler, *Angew. Chem.* **1982,** *94,* 509.

[13] A. A. Bothner-By, R. L. Stephens, J. T. Lee, C. D. Warren, R. W. Jeanloz, *J. Am. Chem. Soc.* **1984,** *106,* 811; A. Bax, D. G. Davis, *J. Magn. Reson.* **1985,** *63,* 207; H. Kessler, C. Griesinger, R. Kerssebaum, K. Wagner, R. R. Ernst, *J. Am. Chem. Soc.* **1987,** *109,* 607.

[14] W. F. Van Gunsteren, H. J. C. Berendsen, *Angew. Chem.* **1990,** *102,* 1020.

[15] A. Di Nola, H. J. C. Berendsen, O. Edholm, *Macromolecules* **1984,** *17,* 2044.

[16] D. Neuhaus, M. P. Williamson, 'The Nuclear Overhauser Effect in Structural and Conformational Analysis', VCH Publishers, New York, 1989; T. L. James, B. Brandon, A. M. Bianucci, N. Zhou, 'NMR and Biomolecular Structure', Eds. I. Bertini, H. Molinari, and N. Niccolai, VCH-Publishers, New York, 1991, 87.

[17] V. F. Bystrov, *Prog. Nucl. Magn. Reson. Spectrosc.* **1976,** *10,* 41.

[18] 'Felix-NMR Data Processing Software, Vers. 2.0', Hare Reasearch Inc., Woodinville, Washington, 1991.

[19] A. Bax, *J. Magn. Reson.* **1988,** *77,* 134.

[20] K. Wüthrich, 'NMR of Proteins and Nucleic Acids', John Wiley & Sons, New York, 1986, p. 162.